Faulty Initiation of Proteoglycan Synthesis Causes Cardiac and Joint Defects

Sevjidmaa Baasanjav,[1,2,14] Lihadh Al-Gazali,[3,14] Taishi Hashiguchi,[4,14] Shuji Mizumoto,[4] Bjoern Fischer,[1] Denise Horn,[1] Dominik Seelow,[1] Bassam R. Ali,[5] Samir A.A. Aziz,[6] Ruth Langer,[7] Ahmed A.H. Saleh,[6] Christian Becker,[8] Gudrun Nürnberg,[8] Vincent Cantagrel,[9] Joseph G. Gleeson,[9] Delphine Gomez,[10] Jean-Baptiste Michel,[10] Sigmar Stricker,[11] Tom H. Lindner,[2] Peter Nürnberg,[8] Kazuyuki Sugahara,[4] Stefan Mundlos,[1,11,*] and Katrin Hoffmann[1,11,12,13,*]

Proteoglycans are a major component of extracellular matrix and contribute to normal embryonic and postnatal development by ensuring tissue stability and signaling functions. We studied five patients with recessive joint dislocations and congenital heart defects, including bicuspid aortic valve (BAV) and aortic root dilatation. We identified linkage to chromosome 11 and detected a mutation (c.830G>A, p.Arg277Gln) in *B3GAT3*, the gene coding for glucuronosyltransferase-I (GlcAT-I). The enzyme catalyzes an initial step in the synthesis of glycosaminoglycan side chains of proteoglycans. Patients' cells as well as recombinant mutant protein showed reduced glucuronyltransferase activity. Patient fibroblasts demonstrated decreased levels of dermatan sulfate, chondroitin sulfate, and heparan sulfate proteoglycans, indicating that the defect in linker synthesis affected all three lines of *O*-glycanated proteoglycans. Further studies demonstrated that GlcAT-I resides in the *cis* and *cis*-medial Golgi apparatus and is expressed in the affected tissues, i.e., heart, aorta, and bone. The study shows that reduced GlcAT-I activity impairs skeletal as well as heart development and results in variable combinations of heart malformations, including mitral valve prolapse, ventricular septal defect, and bicuspid aortic valve. The described family constitutes a syndrome characterized by heart defects and joint dislocations resulting from altered initiation of proteoglycan synthesis (Larsen-like syndrome, B3GAT3 type).

Introduction

Proteoglycans are a major component of connective tissue. They influence the mechanical properties and contribute to regulatory functions including cell proliferation, differentiation, and development.[1–9] The mechanical effect of glycosaminoglycans (GAG) is well understood. Their charge contributes to hydrophilic properties, and the accumulating water ensures an appropriate elastic tissue tonus. In this way, small proteoglycans such as biglycan and decorin help to form and modify collagen fibers in size and organization. Important functions for proteoglycans have been demonstrated for a number of organs including the cardiovascular system. For example, the growth of new blood vessels from pre-existing vasculature is influenced by proteoglycans through modulating the bioactivity of key angiogenic factors such as vascular endothelial growth factor (VEGF(165)) via affecting VEGF's diffusion, half-life, and interaction with its tyrosine kinase receptors.[10,11] Likewise, the differentiation of cardiomyocytes depends on changes in proteoglycan and hyaluronan concentration during differentiation, thereby governing the differentiation of precursor cells to mature functional cells.[12] The importance of these molecules is exemplified by mutations in human disorders such as Simpson-Golabi-Behmel syndrome (MIM 312870), a condition with overgrowth, coarse facies, and a high incidence of congenital heart defects.[13,14] In this case mutations in glypican 3 (*GPC3* [MIM 300037]), the gene encoding a heparan sulfate proteoglycan that binds to the exocytoplasmic surface of the plasma membrane through a covalent glycosylphosphatidylinositol (GPI) linkage, have been described. GPC3 is known to modify the WNT, hedgehog, fibroblast growth factor, and bone morphogenetic protein (BMP) signaling pathways.[14]

Proteoglycans consist of a core protein and glycosaminoglycan side chains. The glycosaminoglycans are attached to serine residues of the core protein via a tetrasaccharide linkage region.[5,15–17] This essential linker region always contains four saccharides (1× xylose [Xyl], 2× galactose [Gal], and 1× glucuronic acid [GlcA]). GAGs are polysaccharides

[1]Institute of Medical Genetics, Charité University Medicine, Augustenburger Platz 1, 13353 Berlin, Germany; [2]Division of Nephrology, Department of Internal Medicine, University Clinic Leipzig, Liebigstr. 20, 04103 Leipzig, Germany; [3]Department of Pediatrics, Faculty of Medicine and Health Sciences, United Arab Emirates University, P.O. Box 17666, Al Ain, United Arab Emirates; [4]Laboratory of Proteoglycan Signaling and Therapeutics, Faculty of Advanced Life Science, Graduate School of Life Science, Hokkaido University, Frontier Research Center for Post-Genomic Science and Technology, West-11, North-21, Kita-ku, Sapporo 001-0021, Japan; [5]Department of Pathology, Faculty of Medicine and Health Sciences, United Arab Emirates University, P.O. Box 17666, Al Ain, United Arab Emirates; [6]Department of Pediatrics, Saqr Hospital, P.O. Box 5450, Ras Al Khaimah, United Arab Emirates; [7]Department of Radiology, Faculty of Medicine and Health Sciences, United Arab Emirates University, P.O. Box 17666, Al Ain, United Arab Emirates; [8]Cologne Center for Genomics (CCG), University of Cologne, Weyertal 115b, 50931 Köln, Germany; [9]Neurogenetics Laboratory, Department of Neurosciences, University of California, San Diego, Leichtag 3A16, 9500 Gilman Drive, La Jolla, CA 92093, USA; [10]INSERM Unit 698, Cardiovascular remodeling, 46, rue Henri Huchard, 75018 Paris, France; [11]Max Planck Institute for Molecular Genetics, Development and Disease, Ihnestraße 63-73, 14195 Berlin, Germany; [12]The Berlin Aging Study II, Research Group on Geriatrics, Charité University Medicine, Reinickendorfer Str. 61, 13347 Berlin, Germany; [13]Institute of Human Genetics, Martin Luther University Halle-Wittenberg, Magdeburger Str. 2, 06112 Halle (Saale), Germany
[14]These authors contributed equally to this work
*Correspondence: stefan.mundlos@charite.de (S.M.), katrin.hoffmann@medizin.uni-halle.de (K.H.)
DOI 10.1016/j.ajhg.2011.05.021.

Table 1. Clinical Features of the Children in This Report

	Patient IV.2	Patient IV.3	Patient IV.4	Patient IV.5	Patient IV.7
Congenital Heart Defects					
Bicuspid aortic valve	-	+	+	+	-
Aortic root dilatation	-	+	+	+	-
Mitral valve prolapse	+	-	+	+	+
Atrial septal defect (ASD)/patent foramen ovale (PFO)	PFO	-	ASD (surgically closed)	PFO	PFO
VSD	-	+	-	-	+
Cranio-facial appearance					
Brachycephaly	+	+	+	+	+
Large prominent eyes	+	+	+	+	+
Downslant palpebral fissures	+	+	+	-	-
Depressed nasal bridge	-	+	+	+	+
Small mouth	+	-	-	+	+
Low set ears	+	-	+	-	-
Small/dysmorphic ears	+	+	+	-	-
Micrognathia/microretrognathia	+	-	+	+	+
Short/webbed neck	+	+	+	+	+
Skeletal Abnormalities					
Short stature	<P3[a]	<P3	<P3	P3	P3
Dislocated joints	elbow	elbow	shoulder, elbow, prox. radioulnar	elbow	elbow
Joint laxity (wrist and interphalangeal)	+	+	+	+	+
Elbow joint contractures	+	+	+	+	+
Broad ends of fingers and toes	+	+	+	+	+
Foot deformity (talipes varus, metatarsus varus, and flat feet)	+	+	+	+	+

All patients had heart and/or aortic disease as well as distinct skeletal abnormalities, including short stature and multiple joint dislocations together with variable degree of facial dysmorphic features.
[a] P percentile.

that are composed of repeating disaccharide units consisting of an amino sugar (*N*-acetylglucosamine [GlcNAc] or *N*-acetylgalactosamine [GalNAc]) and an uronic acid (GlcA or iduronic acid [IdoA]). The composition of the GAG chain defines the nature of the proteoglycan. Additional disaccharide repeat units of *N*-acetylglucosamine and glucuronic acid $[GlcNAc\text{-}GlcA]_n$ produce heparans, whereas repeats of *N*-acetylgalactosamine and glucuronic acid $[GalNAc\text{-}GlcA]_n$ produce chondroitins. Modifications such as sulfation and epimerization further increase the structural and functional diversity of proteoglycans (see Figure S1 available online). The synthesis of the proteoglycan linker region is a complex specialized process that involves several enzymatic steps (see Figure S1 for details).

Here we describe a family with a distinct recessive phenotype, consisting of small stature, joint dislocations, and congenital heart defects including bicuspid aortic valve and mitral valve prolapse. We identified mutations in *B3GAT3* (MIM 606374; ENA database AAH71961), the gene encoding glucuronyltransferase-I (GlcAT-I) that adds the last component of the linker region. The mutation causes a drastic reduction of GlcAT-I activity and results in the production of immature dermatan sulfate (DS) proteoglycans as well as in a reduced number of chondroitin sulfate (CS) and heparan sulfate (HS) chains. We describe a syndrome caused by impaired proteoglycan maturation, providing evidence that normal side chain synthesis is essential for the development of the heart, in particular its valves, and the skeleton. We suggest naming it Larsen-like syndrome, B3GAT3 type.

Material and Methods

Patients

We studied a consanguineous family with five affected children (Table 1, Figures 1 and 2, Figure S2). All members of the family

Figure 1. Mutations in *B3GAT3* Are Associated with a Specific Phenotype

(A) Facies appeared flattened with large eyes, hypertelorism, long and downslanting palpebral fissures, depressed nasal bridges, and micrognathia. Note dislocation of elbow, broad fingers and toes, and foot deformity.

(B) Radiographs show dislocation of shoulder, elbow, and proximal radio-ulnar joints. Mild shortening of metacarpal bone I, pseudoepiphysis at the second metacarpal bone, dissociation and retardation of the bone age, and mild irregularities at several metaphyses are shown.

(C) Echochardiography showing aortic dilation and bicuspid aortic valve.

Numbers in left lower corner indicate the patient's ID corresponding to the pedigree and Table 1.

were clinically assessed and individual organ systems studied to ascertain the full phenotype. The study has been approved by the Charité University medicine, United Arab Emirates University, and Hokkaido University ethics committees. The procedures followed were in accordance with the ethical standards of the responsible committees on human experimentation (institutional and national). Written, informed consent was obtained from all participants or their legal guardians.

Genomic and Molecular Analysis

Genotyping was performed with the 10 k Affymetrix SNP chip. The data were analyzed with ALLEGRO v1.2c, GENEHUNTER v2.1r5 under the graphical user-interface easyLINKAGE v5.08.[18,19] A recessive model with complete penetrance, disease allele frequency of 0.001, and equally distributed marker alleles was assumed. Fine mapping with microsatellites was done as previously described.[20] We included all available family members and reconstructed haplotypes by GENEHUNTER and manually.

We sequenced functional candidate genes within the linkage interval by standard sequencing procedures. Functional candidates were selected based on their expression potential function and/or previously reported skeletal and cardiac phenotypes in human or animal models, respectively, in the gene itself or associated pathway genes and interaction partners. Primer sequences of used microsatellite markers and sequenced genes are available upon request. The mutation was tested in controls (147 population-matched controls and 425 blood donors of European descent) and for correct segregation within the patient's family.

All coding sequences and flanking intron regions of *B3GAT3* (GlcAT-I, NM_012200.2, GI:12408653; NP_036332.2) were amplified and sequenced by standard protocols. Primer sequences are provided in Table S1.

Quantitative PCR

B3GAT3 mRNA levels were studied in different tissues and cell lines by quatitative PCR (qPCR). After cell lysis with Trizol and standard phenol/chloroform RNA extraction, total cDNA was transcribed by RevertAid H Minus First Strand cDNA Synthesis Kit (Fermentas, Burlington, Ontario, Canada). For qPCR on ABI Prism 7500 (Applied Biosystems, Foster City, CA), we mixed cDNA, SYBR Green (Invitrogen, Carlsbad, Ca), and primers (primer sequences in Table S1). We analyzed qPCR data with the ABI Prism SDS Software package (ΔΔCt method; normalization against *GAPDH*).

To determine the expression levels of decorin mRNA, total RNA was extracted from fibroblasts of each subject and cDNAs were synthesized with reverse transcriptase by standard protocols. The quantitative real-time RT-PCR was performed by Mx3005P (Stratagene, La Jolla, CA) with decorin-specific primer pairs (primer sequences in Table S1).

Molecular Modeling

The model used was the X-ray structure of the human GlcAT-I bound to UDP-GlcA. The Protein Data Bank code for this model is 1KWS and is available at the RCSC protein data bank. The result of the modeling was rendered with PyMol.

Glucuronyltransferase Activities of WT and Mutant GlcAT-I

UDP-[^{14}C]GlcA (180.3 mCi/mmol) was purchased from Perkin-Elmer Life and Analytical Sciences (Boston, MA). A human

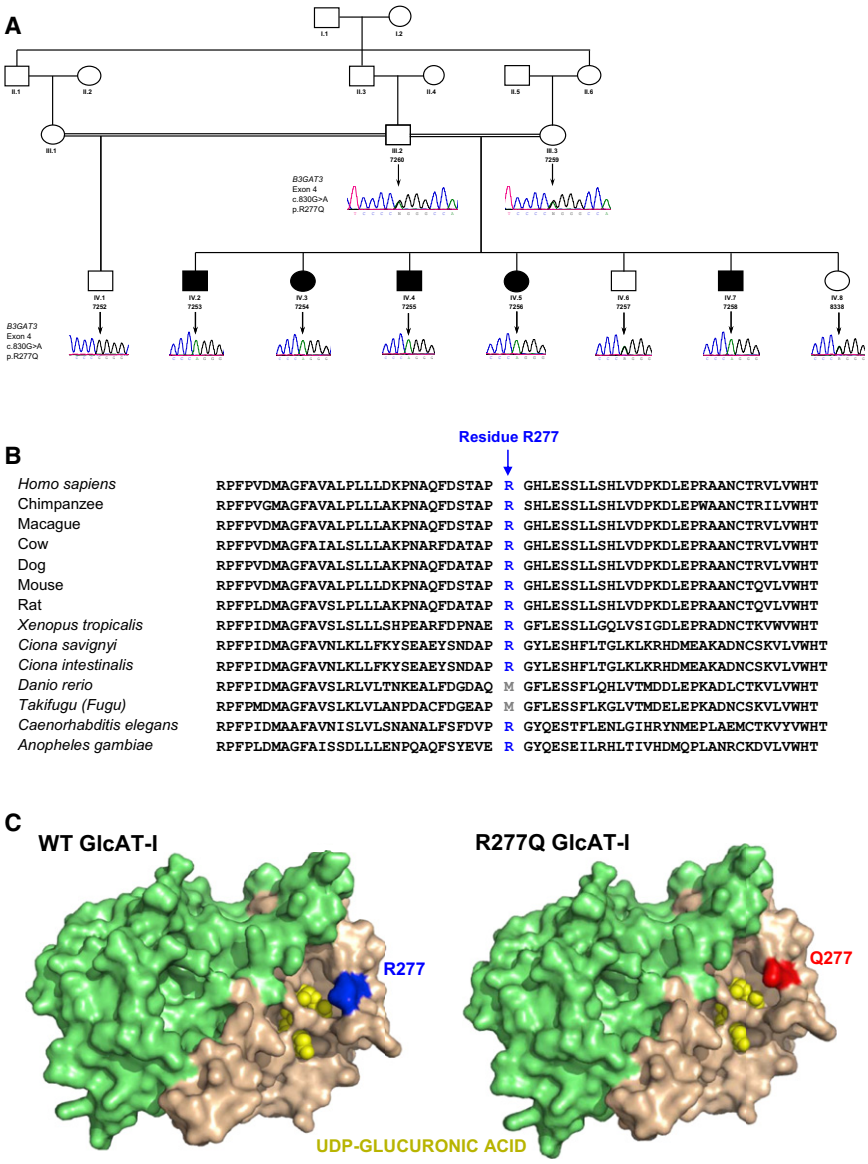

Figure 2. Molecular Analysis
(A) Pedigree of the family. All affected family members are homozygous for the mutation c.830G>A in exon 4 of the *B3GAT3* gene.
(B) Residue p.Arg277 (p.R277) is evolutionary conserved.
(C) *B3GAT3* encodes the glucuronyltransferase GlcAT-I that functions as a dimer (light green and light brown).[32,45] Residue p.Arg277 (p.R277, blue) is involved in substrate interaction and is critical for binding the substrate GlcA. Note that the side chain of p.Arg277 (p.R277) is close to the carboxyl group at the C-5 position of GlcA but is further away in the mutant p.Gln277 (p.Q277). (Modeling used Protein Data Bank file lKWS for the crystal structure of GlcAT-I interacting with the substrate UDP-glucuronic acid [UDP-GlcA].)

GlcAT-I/pOTB7 vector (IMAGE Consortium cDNA clone, ID number 4299539) was purchased from Open Biosystems Inc (Huntsville, AL). Anti-FLAG M2 affinity resin, anti-FLAG Monoclonal antibody, Galβ1-3Galβ1-*O*-methyl, and p3XFLAG-CMV8 vector were purchased from Sigma (Saint Louis, MO). An ECL advance western blotting detection kit and Hybond-P membranes were purchased from GE Healthcare (Buckinghamshire, UK). FuGENE 6 transfection reagent was purchased from Roche Diagnostics (Basel, Switzerland). Restriction enzymes were purchased from New England Biolabs (Hitchin, UK). *KOD*-Plus DNA polymerase was purchased from Toyobo (Tokyo, Japan). AG 1-X8 resin (100–200 mesh) was purchased from Bio-Rad (Hercules, CA).

The expression vector of human GlcAT-I was constructed as described previously.[21,22] In brief, a truncated form of GlcAT-I (wild-type), lacking the first NH_2-terminal 43 amino acids of the GlcAT-I, was amplified by PCR with a 5′ primer containing an in-frame EcoRI site (5′-GCGAATTCACTACGGCAGAAGGAT-3′) and a 3′ primer containing a SalI site located 71 bp downstream of the stop codon (5′-GCGTCGACGAAAACCACATCCT-3′) and hGlcAT-I/pOBT7 as a template. We carried out two rounds of PCR for the construction of the amino acid-substituted mutant of GlcAT-I (p.Arg277Gln). The first PCR was performed with a 5′ primer containing an in-frame EcoRI site (5′-GCGAATTCACT ACGGCAGAAGGAT-3′) and a 3′ internal mutagenic oligonucleotide primer (5′-CA GGTGGCCCTGGGGAGCGGTGGA-3′), 5′ internal mutagenic oligonucleotide primer (5′-TCCACCGCTCCCCAGGGCCACCTG-3′), and 3′ primer containing a SalI site (5′-GCGTCGACGAAAACCACATCCT-3′) and hGlcAT-I/pOBT7 as a template (underlining indicates modified nucleotides). The second PCR was performed with a 5′ primer containing an EcoRI site (5′-GCGAATTCACTACGGCAGAAGGAT-3′), 3′ primer containing a SalI site located 71 bp downstream of the stop codon (5′-GCGTCGACGAAAACCACATCCT-3′), and the first PCR products as a template. PCR was carried out with *KOD*-Plus DNA polymerase by 30 cycles of 94°C for 30 s, 55°C for 42 s, and 68°C for 60 s. The amplified fragments were digested with EcoRI and SalI and inserted into p3XFLAG-CMV8.

The expression plasmid (6.7 μg) was transfected into COS-7 cells (Japan Health Sciences Foundation, Tokyo, Japan) on a 100 mm dish with FuGENE 6 according to the instructions provided by the manufacturer. Three days after transfection, 0.25 ml each of the culture medium was collected and incubated with 10 μl of anti-FLAG M2 affinity resin overnight at 4°C. The beads were recovered by centrifugation and washed with 1 ml of 50 mM Tris-HCl (pH 7.5) containing 150 mM NaCl, 0.05% Tween 20, and then resuspended in the assay buffer for enzyme activity.

The culture medium (0.2 ml) was incubated with 10 μl of anti-FLAG M2 affinity resin overnight at 4°C. The beads were recovered by centrifugation, washed with TBST, and then analyzed on a 12.5% sodium dodecyl sulfate (SDS)-polyacrylamide gel, transferred to a polyvinlidene difluoride (PVDF) membrane, and incubated for 1 hr with FLAG antibody. The bound antibody was

detected with anti-mouse IgG conjugated with horseradish peroxidase.

Enzyme Assay of the Recombinant WT and Mutant GlcAT-I

The glucuronyltransferase assay mixture contained 10 μl of the resuspended anti-FLAG affinity resins/50 mM 2-(*N*-morpholino) ethanesulfonic acid-NaOH (pH 6.5)/171 μM ATP/10 mM $MnCl_2$/14.3 μM UDP-[^{14}C]GlcA (1.77 × 10^5 dpm)/60 nmol Galβ1-3Galβ1-*O*-methyl as acceptor substrate in a total volume of 30 μl. The reaction mixture was incubated at 37°C for 1 hr. The ^{14}C-labeled products were isolated by applying the reaction mixture onto a tiny tip column packed with AG 1-X8 resin (a PO_4^{2-} form, 100–200 mesh) to remove excess UDP-[^{14}C]GlcA.[23] The isolated products were quantified in a liquid scintillation counter (LS6500, Beckman coulter).

Comparison of the GlcAT-I Activities of Fibroblast Homogenates from Patients and Age-Matched Controls

The following fibroblasts were used for the assay. Age-matched controls for patient A820 (male, 11 years old) were GM03348E (male, 10 years old) and AG16409 (male, 11 years old). Age-matched controls for patient A821 (male, 17 years old) were GM07492A (male, 17 years old) and GM07753 (male, 17 years old). The homogenates of the fibroblasts were assayed with Galβ1-3Galβ1-*O*-methyl as an acceptor (220 nmol) and UDP-[^{14}C]GlcA as a donor substrate, and then incubated for 4 hr at 30°C.

Immunofluorescence

For immunofluorescence analysis, the cells were washed three times in phosphate-buffered saline (PBS), fixed in 4% paraformaldehyde for 10 min at 4°C, and permeabilized in 3% BSA in 1× PBS with 0.4% Triton X-100 for 10 min at 4°C. GlcAT-I protein was detected by a mouse anti-GlcAT-I polyclonal antibody (Abnova, Taipei, Taiwan: H00026229-B01P). For testing the colocalization analysis with Golgi proteins, we used sheep anti-GM130 (kind gift by Francis A. Barr), rabbit anti-Giantin (Covance, Princeton, NJ), and sheep anti-TGN46 (Serotec, Oxford, UK). As secondary antibodies we applied anti-mouse IgG Alexa Fluor 555 (Invitrogen, Molecular Probes) and an anti-sheep/rabbit IgG Alexa Fluor 488 (Invitrogen, Molecular Probes) conjugates. We stained DNA by DAPI and mounted cells in Fluoromount (Scientific Services, Cornwall, UK). Images were collected with an LSM 510 meta (Carl Zeiss, Göttingen, Germany) with a x63 Plan Apochromat oil immersion objective.

Immunoblotting of Aortic Media Extracts

Normal walls of the ascending aorta and aortic arch were obtained in healthy subjects at the time of organ collection for heart/lung transplantation with the authorization from the French Biomedicine Agency. Protein extractions were performed directly from frozen aortic media (after the separation from intima and adventitia) and stored at −80°C. The media preparations were pulverized in liquid nitrogen, using a freezer mill (model 6750 SPEX SamplePrep, Metuchen, NJ), and subsequently homogenized in a hypotonic lysis buffer (50 mM Tris [pH 8], 150 mM NaCl, 1% Triton X-100, 1% sodium deoxycholate, 5 mM EDTA) containing a cocktail of protease and serine/threonine and tyrosine phosphatase inhibitors (Sigma). The protein concentration from each sample was determined and extracts were separated by 10% SDS-polyacrylamide gel electrophoresis. Proteins were transferred to a PVDF membrane, blocked with 5% BSA-TBS-T (Tris-buffered saline [pH 7.4]-0.1% Tween 20) for 1 hr. Membranes were then incubated overnight (4°C) with primary antibodies: polyclonal B3GAT3 (1 μg/ml, Abnova), monoclonal B3GAT3 (1 μg/mL, Abnova), or GAPDH (1.6 μg/ml, Biovalley, Freiburg, Germany). Membranes were then washed with TBS-T and incubated with anti-mouse IgG (Jackson Laboratories, Bar Harbor, ME) for 1 hr. The signal was detected with a chemiluminescence kit (ECL Plus kit; Amersham).

Analyses of Dermatan Sulfate, Chondroitin Sulfate, and Heparan Sulfate Proteoglycans in Patient and Control Fibroblasts

The serum-free conditioned medium of the cultured fibroblasts of control subjects and patients was collected and concentrated with Amicon Ultra-4 (Ultracel-30k, Millipore, Billerica, MA). An aliquot of the medium (5 μg as total protein) was digested with a highly purified (protease-free) chondroitinase (CSase) ABC (EC 4.2.2.20, Seikagaku Corp., Tokyo, Japan), and each digest was subjected to SDS-polyacrylamide gel electrophoresis. Western blotting was carried out with an anti-human decorin antibody (clone 115402, R&D Systems, Minneapolis, MN) and an ECL advance detection kit (GE healthcare).

For determination of the number of CS and HS chains, cultured fibroblasts from patients and control subjects (age and sex matched) were collected and washed with PBS. The cells were treated with CSase or a mixture of heparinases (HSases) -I (EC 4.2.2.7) and -III (EC 4.2.2.8) (IBEX Technologies, Montreal, Canada) at 37°C for 1 hr. After washing with PBS, CSase- or HSase-treated cells were individually incubated with the primary antibodies, anti-CS-stub (2B6) and anti-HS-stub (3G10) (Seikagaku Corp.), and subsequently the cells were incubated with the Alexa Fluor 488-labeled anti-mouse IgM secondary antibody (Molecular Probes, Eugene, OR). Incubation of the fibroblasts with the secondary antibody alone was also performed as a negative control experiment. Alexa Fluor 488-bound cells were analyzed by immunofluorescence flow cytometry in a BD FACSCanto (BD Biosciences, San Jose, CA).

Results

Patients' Phenotype Defines a Syndrome Characterized by Joint Dislocations and Congenital Heart Defects Including Bicuspid Aortic Valve

The parents were first cousins with five affected and two unaffected children (Figures 1 and 2, Figure S2, Table 1). All five patients had congenital heart defects in variable combinations (Figure 1C, Table 1). Bicuspid aortic valve with dilatation of the aortic root was present in three, mitral valve prolapse in four, patent foramen ovale in three, and ventricular septal defect in two of the patients. All affected children had short stature (height < 3%) and presented variable craniofacial dysmorphic features which included brachycephaly, thick eyebrows, large eyes with downslanting palpebral fissures, depressed nasal bridge, narrow mouth, and micrognathia or microretrognathia. The ears in some of them were small, low set with prominent antitragus, and slight uplift of the lobe. The neck was short (webbed in IV.2) with low posterior hair line. There was mild chest asymmetry.

In addition, all affected individuals had congenital dislocations and contractures of the elbow joint as well

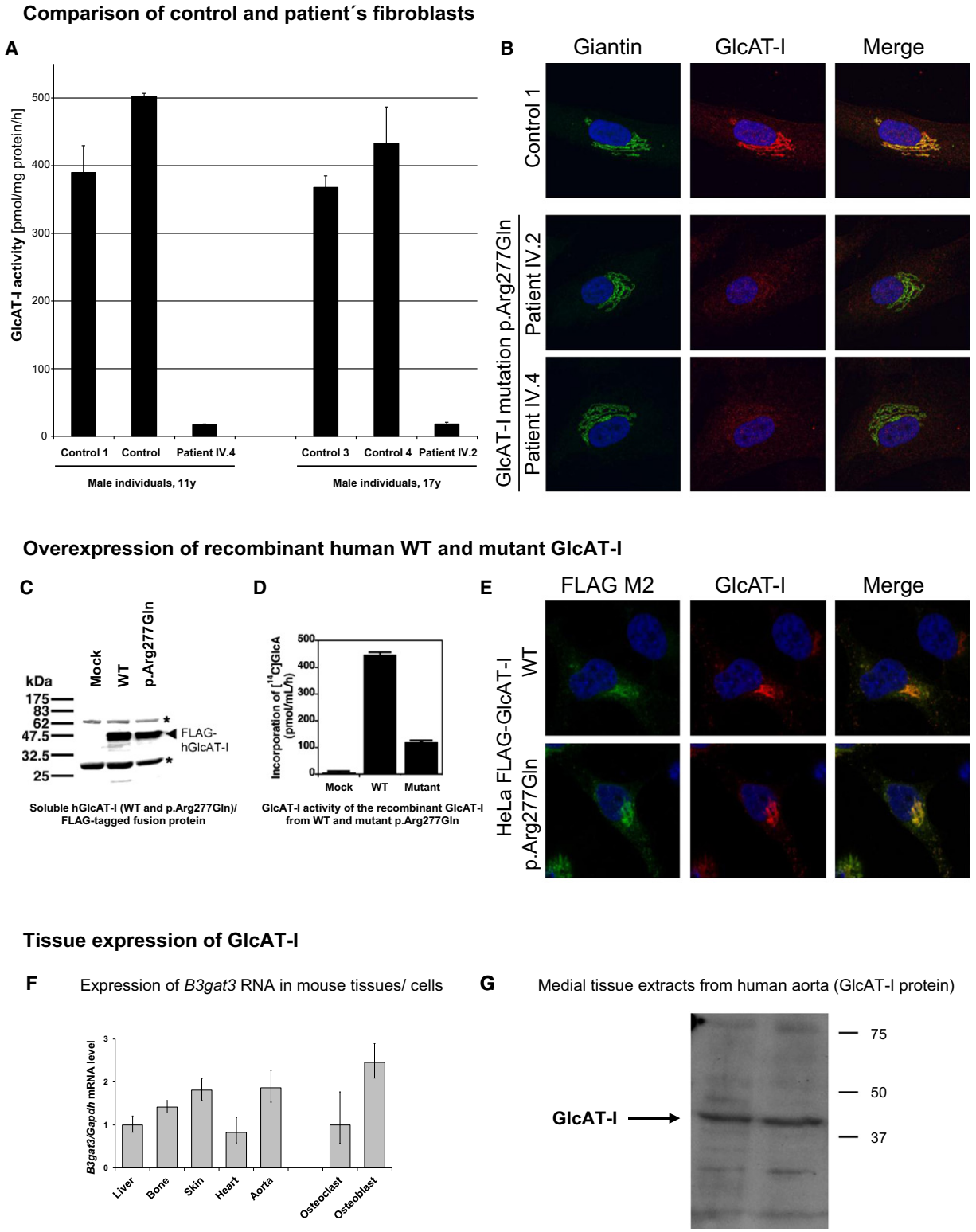

Figure 3. Expression and Activity of GlcAT-I

(A) GlcAT-I activity in fibroblasts is markedly reduced in patients compared to age-matched controls. The homogenates of the fibroblasts were assayed with Galβ1-3Galβ1-*O*-methyl as an acceptor (220 nmol) and UDP-[^{14}C]GlcA as a donor substrate, and then incubated for 4 hr at 30°C. The results are from duplicate experiments. Unit is pmol/mg protein/hr.

(B) Reduced amount of mutant GlcAT-I and loss of Golgi localization in patient's fibroblasts. By comparison, GlcAT-I (red) colocalizes with the *cis* and *cis*-medial Golgi marker GIANTIN (green) in wild-type fibroblasts.

(C and D) Glucuronyltransferase activities of the human recombinant GlcAT-I (WT and p.Arg277Gln) showed similar amounts of proteins (C) but reduced activity by mutation p.Arg277Gln (D).

as talipes equinovarus and/or metatarsus varus. Joint dislocations were also observed in the shoulders. Joint laxity was present in the wrists and interphalangeal joints. The finger tips and the hallux on both sides appeared wide. Radiographs showed dislocations of the shoulder, elbow, and proximal radial-ulnar joints (Figure 1), a mild shortening of the first metacarpal bone, delayed and dissociated bone age (~4 years at the chronological age of 8 years), mild dysplasia of the hip joints, and foot deformities. The vertebral column showed signs of osteopenia; several vertebrae were already flattened. The children had a normal mental and motor development.

Disease Mapping and Identification of the Disease-Causing Mutation in *B3GAT3*

We performed genome-wide linkage analyses and mapped the disease to chromosome 11q12 (multipoint LOD = 3.76; Figure S3A). Fine mapping narrowed the region to an 8 cM interval (final multipoint LOD = 3.89; Figure S3B) containing 262 genes. We sequenced 30 functional candidate genes within this region (Table S2). We identified the homozygous missense mutation c.830G>A in *B3GAT3*, the gene encoding the enzyme beta-1,3-glucuronyltransferase 3 (GlcAT-I), which resulted in the substitution of arginine at position 277 by glutamine (p.Arg277Gln). The mutation p.Arg277Gln segregated with the disease in the family (Figure 2A) and was present neither in 294 chromosomes from population-matched controls nor in 850 chromosomes from Berlin blood donors. Residue p.Arg277 is evolutionary highly conserved and alters a functionally important domain involved in substrate interaction, especially in binding the substrate GlcA (Figures 2B and 2C).

Reduced GlcAT-I Enzyme Activity in Patient Cells

The p.Arg277 residue has previously been shown to be essential for enzymatic activity in a mutagenesis experiment (p.Arg277Ala) by ensuring GlcAT-I substrate specificity.[24] We therefore reasoned that the mutation p.Arg277Gln might have a similar effect on GlcAT-I activity. Our studies in the homogenates from patient-derived fibroblasts demonstrated that the missense mutation p.Arg277Gln results in a significant reduction of glucuronyltransferase activity. GlcAT-I activity in patient fibroblasts (patients IV.2 and IV.4) was reduced to 3%–5% of age-matched control levels (Figure 3A). Thus, mutant cells showed a drastic reduction in GlcAT-I activity but still showed some basal activity, indicating that the mutation is hypomorphic.

By using immunofluorescence and colocalization with Golgi-marker proteins, we showed that GlcAT-I is located in the *cis* and *cis*-medial Golgi (Figure S4). In mutant cells the protein level is dramatically reduced (Figure 3B). We tested whether the antibody detects both the wild-type and the mutant protein and found that the mutation did not affect antibody binding (Figure S5), whereas mutation c.830G>A did not significantly reduce the level of *B3GAT3* mRNA (data not shown). These observations suggest that the mutant GlcAT-I protein might have been degraded or produced to a lesser extent as compared to the wild-type. As previously shown, artificially introduced missense mutations can reduce enzymatic activity and secondarily decreased stability of the mutant, dysfunctional enzyme by ER retention and subsequent proteasomal decay.[25]

To test whether the mutation p.Arg277Gln indeed reduces GlcAT-I activity by impaired enzymatic function and not by primary reduced protein level, we transfected cells with the human GlcAT-I wild-type and the mutated (p.Arg277Gln) vector. We found a marked reduction of GlcAT-I activity in the mutant despite similar amounts of the wild-type and mutant proteins (Figures 3C–3E), suggesting that the reduced enzymatic activity of GlcAT-I affects protein stability.

Expression of *GlcAT-I* in Heart, Aorta, and Bone

Individuals with the c.830G>A mutation showed heart defects, aortic root dilatation, and skeletal malformations. Reverse-transcriptase quantitative PCR on corresponding mouse tissues demonstrated that *B3GAT3* mRNA is expressed in heart, aorta, bone, and also in osteoblasts (Figure 3F). In addition, GlcAT-I protein was present in human aorta (Figure 3G).

GlcAT-I Mutations Are Associated with Immature DS Proteoglycans as well as with Reduced Amounts of CS and HS Chains in Patient Cells

We tested how the reduced enzyme activity affects the products of proteogylcan synthesis. The overall amount

(C) For western blotting, the purified recombinant FLAG-GlcAT-I (WT and p.Arg277Gln) was separated by 12.5% SDS-polyacrylamide gel electrophoresis and detected with the FLAG M2 antibody. The arrowhead and asterisks indicate the recombinant enzyme and the light and heavy chains of the antibody, which is derived from the anti-FLAG agarose resin used for purification, respectively.
(D) Catalytic GlcAT-I activity of the recombinant enzyme (p.Arg277Gln) was reduced compared to the wild-type. Activities represent the averages and standard error of two independent experiments, which were performed in duplicate. Mock indicates the glucuronyltransferase activity obtained with the conditioned medium transfected with an empty vector as a control. Experiments were performed at 37°C.
(E) The GlcAT-I antibody (Abnova) recognizes both the wild-type and the mutant recombinant GlcAT-I, thus excluding preferential antibody binding to the wild-type. (Western blotting in Figure S5.)
(F) RNA-expression of *B3gat3* in different disease relevant tissues (obtained from newborn black 6 mice [C57BL/6], postnatal day P4) as well as from osteoblast and osteoclast cell cultures. Data were obtained from three different experiments (error bars represent standard error of the mean [SEM]).
(G) Western blotting of GlcAT-I in human aorta. Western blotting shows presence of GlcAT-I in medial tissue extracts from human wild-type aorta.

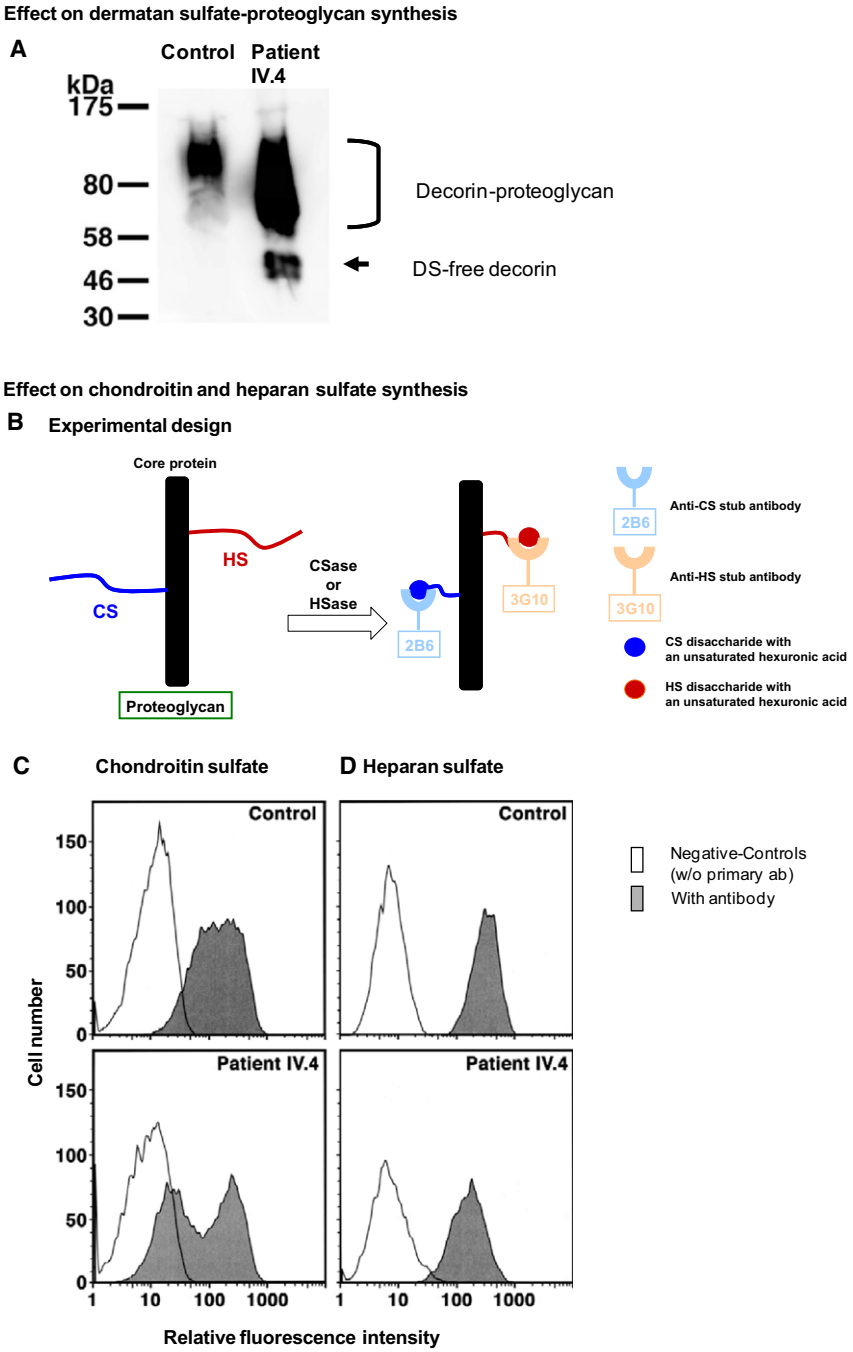

Figure 4. Effect of GlcAT-I Mutations on DS, CS, and HS Proteoglycan Synthesis

(A) DS-free decorin is detected in patient but not in control fibroblasts, indicating an insufficient dermatan sulfate synthesis. Western blotting of a DS-proteoglycan, decorin, produced by fibroblasts. The conditioned medium derived from wild-type fibroblasts showed a broad band of decorin-proteoglycan around 60–120 kDa. In contrast, the conditioned medium derived from the patient fibroblasts revealed two bands. The upper band represents decorin-proteoglycan with a DS chain. The lower band ~50 kDa is predicted to be decorin with only the linkage region trisaccharide (Gal-Gal-Xyl), without a DS chain. These observations suggest that the mutation p.Arg277Gln in GlcAT-I is associated with insufficient synthesis of dermatan sulfate proteoglycan.
Control: age-, sex-, and population-matched (male, 11 years old, AG16409); patient IV.4: male, 11 years old (mutation p.Arg277Gln in GlcAT-I, A820). The arrow indicates DS-free decorin.
(B) Experimental design for analyzing CS and HS synthesis. The unsaturated hexuronic acid containing CS and HS, which were generated by the treatment with CSase or HSase, are recognized by the anti-CS-stub and anti-HS-stub antibodies, respectively.
Anti-stub CS (2B6) and anti-stub HS (3G10) antibodies can recognize the unsaturated hexuronic acid-containing oligosaccharide that are generated by the treatment with bacterial CSase and HSase, respectively, whereas neither intact CS nor HS can be recognized. Therefore, these antibodies can be used as probes for investigating the *relative* number of CS and HS chains on the core proteins of proteoglycans. It should be noted that the truncated GAG-protein linkage trisaccharide Gal-Gal-Xyl- expressed on core proteins in the GlcAT-I mutant cells is not recognized by either antibody.
(C and D) Analysis of the relative number of CS and HS chains expressed on the cell surface of fibroblasts by flow cytometry. To examine the expression of CS and HS on the cell surface, the fibroblasts from the 11-year-old patient IV.4 and from controls (AG16409) were treated with CSase and then with anti-stub 2B6 antibodies (C) or HSase and then with anti-stub 3G10 antibodies (D), respectively. The binding of these antibodies to the epitopes on the cell surface was visualized by flow cytometry after incubating with Alexa Fluor 488-conjugated secondary antibody. The gray and white histograms show the intensity of the fluorescence with or without anti-stub antibody, respectively. Similar results were also obtained with those from the 17-year-old patient IV.2 (Figure S6B).

of GAGs in fibroblasts from patients did not show an obvious decrease compared to that of age-matched controls (data not shown). Next we analyzed the proteoglycan decorin in fibroblasts from patients by western blotting. Decorin is secreted by fibroblasts and has a single DS chain when proteoglycan synthesis is undisturbed. We detected DS-free decorin in the patients' cells but not in control fibroblasts (Figure 4A; Figure S6), suggesting that the mutation p.Arg277Gln in GlcAT-I results in the production of the immature DS-proteoglycan decorin.

We examined specifically decorin proteoglycan by western blotting by using the conditioned media from fibroblasts of patients IV.2 and IV.4. One broad-band of decorin-proteglycan (around 80 kDa) was detected in control fibroblasts. In contrast, we detected two bands in fibroblasts from both patients (Figure S6A, lanes 3 and 6). The upper band was decorin proteoglycan with a DS chain as

shown in the wild-types (Figure S6A, lanes 1, 2, 4, and 5), whereas the lower band (~50 kDa) is predicted to be DS-free decorin with the linkage region trisaccharide stub, Galβ1-3Galβ1-4Xyl, where Gal and Xyl stand for D-galactose and D-xylose, respectively. Furthermore, the lower band corresponded to the band observed for the conditioned medium treated with CSase ABC (Figure S6). Thus, the lower band in patients was most probably the signal of DS-free decorin. These observations suggest that the mutation of GlcAT-I (p.Arg277Gln) was responsible for the lack of a DS chain on the core protein.

Based on the result from western blotting of decorin, the amount of its core protein seemed to be upregulated. Therefore, we analyzed the expression level of decorin mRNA by quantitative RT-PCR. Interestingly, the mRNA levels of decorin were 3- to 4-fold increased in patients compared to control fibroblasts (Figure S7), indicating that decorin mRNA levels might be upregulated to compensate for the immature decorin.

Next we examined the synthesis of CS and HS chains on the surface of fibroblasts from patients and age- and sex-matched controls by flow cytometry with CS-stub and HS-stub antibodies (Figures 4B–4D; Figure S6B). The 2B6 antibody, which recognizes the oligosaccharides containing the unsaturated hexuronic acid after treatment with CSase, showed a markedly reduced binding to the epitopes on the patient cells relative to those of the control subject (Figure 4C), showing a bimodal distribution of the cells. To quantify the relative amounts of the CS chains, the mean fluorescence intensity (MFI) of the cell population stained with 2B6 was used. The MFI value for the patient IV.4 was 6.0 (65%) as compared with 9.2 of the age-matched control subject. The 3G10 antibody, which recognizes the oligosaccharides containing the unsaturated hexuronic acid after the treatment with HSase, also showed a reduced binding to the epitopes on the patient cells relative to those of the control subject (Figure 4D). The MFI value after staining with 3G10 was 21.4 (53%) for the patient IV.4 as compared with 40.3 for the age-matched control subject. Similar results were obtained for the fibroblasts from patient IV.2 (Figure S6B). These differences in the MFI values correspond to those of the numbers of the CS and HS chains at cell surface of the control and the patient cells. Namely, the number of the CS and HS chains was reduced to 65% and 53% of the control, respectively. The bimodal distribution of the cells from the 11-year-old male patient (Figure 4C) suggests two different cell populations, one with a reduced number of GAG polysaccharides most probably with a trisaccharide stub (Gal-Gal-Xyl), and the other with a larger number of GAG polysaccharides. Interestingly, the same seems to be true for the fibroblasts from the 17-year-old normal subject (Figure S6B). A possibility is the age-dependent bimodal cell population with a smaller and a larger number of GAG polysaccharides, which remains to be investigated.

These results suggest that the mutant GlcAT-I cannot transfer GlcA to a significant portion of the linker region trisaccharide Gal-Gal-Xyl, resulting in the partial deficiency of all three lines of *O*-glycanated proteoglycans (CS, HS, and DS proteoglycans).

Discussion

We describe a family with recessive inheritance of heart and/or aortic disease as well as of distinct skeletal abnormalities (short stature, multiple joint dislocations) and variable cranio-facial dysmorphic features (Larsen-like syndrome, B3GAT3 type).

There are some similarities to otopalatodigital syndrome type II (OPD2 [MIM 304120]), particularly the downslanting palpebral fissures, narrow mouth, contractures at the elbows, and broad fingertips and hallux. However, the radiological changes in OPD2 are different and the inheritance is X-linked recessive rather than autosomal recessive. Short stature, short webbed neck, and the facial appearance of the children in this report could also suggest Noonan syndrome. Nevertheless, the presence of joint dislocations and the recessive pattern of inheritance in this family made this diagnosis unlikely. Absence of the typical radiological changes seen in Desbuquois syndrome (DBQD [MIM 251450]) in this family ruled this diagnosis out. We also considered the classic Larsen syndrome (LRS [MIM 150250]) caused by dominant FLNB (MIM 603381) mutations particularly because there are multiple joint dislocations, broad fingertips, and hallux but the facial appearance is different, the bone age is delayed rather than advanced, and the inheritance is recessive in our family. There are also many similarities of the family in this report to the autosomal-recessive Larsen syndrome, CHST3 type. This disorder includes a spectrum of phenotypes ranging from Larsen syndrome, humerospinal dysostosis, chondrodysplasia multiple dislocations, and spondylo-epiphyseal dysplasia, Omani type.[26–28] Children present at birth with reduced length and multiple joint dislocations. During childhood, the dislocations improve and features of SED-OT appear. These features include intervertebral disc degeneration, rigid kyphoscoliosis, and trunk shortening. The bone age is also delayed. There are usually vertebral changes on lateral X-ray of the spine. These include superior and inferior notching reminiscent of a partial coronal cleft.[26] Involvement of the heart valves in this disorder has also been reported. There are no vertebral changes on radiological examination in our family and clinically the older children in our family (now 17, 14, and 13 years old) have no kyphoscoliosis or trunk shortening. However, differentiation between these two disorders is difficult in infancy and early childhood. The combination of brachycephaly, downslanting palpebral fissures, retrognathia, and abnormal ears with club feet, hypermobility of the joints of the hands, shoulders, and feet together with congenital heart disease raised the possibility of musculocontractural EDS (previously known as adducted thumb-clubfoot syndrome and EDS type VIB),

which is caused by mutations in *CHST14*.[29–31] However, the children in this report have normal build and skin with no delay in wound healing and no contractures of the fingers.

Here we describe that mutations in *B3GAT3*, the gene coding for GlcAT-I, result in a condition characterized by congenital dislocations, short stature, and heart defects including bicuspid aortic valve. GlcAT-I functions as a dimer of two subdomains with donor and acceptor specificity.[32] The active sites resides in a cleft between the two chains in which the new incoming saccharide is oriented, chemically reduced, and eventually fused to the already established trisaccharide linker.[32,33] Ouzzine et al. used in vitro mutagenesis to test which residues define the substrate specificity of GlcAT-I. They identified residue 277 (mutagenesis p.Arg277Ala) as important and concluded that the arginine at position 277 is essential for GlcAT-I substrate specificity.[24,34] Our studies in a recombinant cell system as well as in the homogenates from patient-derived fibroblasts demonstrated that the missense mutation p.Arg277Gln significantly reduces the glucuronyltransferase activity (GlcAT-I). Nevertheless, cells with mutant GlcAT-I had residual basal activity in the patient fibroblasts and in vitro, indicating that the mutated protein is still able to function.

We show that reduced GlcAT-I activity affects major components of the extracellular matrix, resulting in immature DS proteoglycans as well as in a reduced number of CS and HS chains in patient cells. The mutation affects the final step in the synthesis of the tetrasaccharide linker region, which is required for initiation of GAG side chain synthesis of proteoglycans. Our data demonstrate that GlcAT-I is located in the *cis* and *cis*-medial Golgi. This is consistent with the catalytic function in glycosylation of the Golgi apparatus and the identification of the GlcAT-I rat ortholog in an endoplasmic reticulum (ER)/Golgi proteomics screening perfomed in rat liver homogenates.[35]

We found that an impairment of GlcAT-I function affects the synthesis of CS, DS, and HS. DS-free decorin proteoglycans were present in the patient fibroblasts but not in controls. These results suggest that the GlcAT-I mutation p.Arg277Gln results in the synthesis of immature proteoglycans, i.e., GAG-free proteoglycans such as DS-free decorin. Interestingly, the synthesis of the decorin core protein was upregulated, probably to compensate for the dysfunctional decorin. In addition, mutant cells showed an apparent reduction in the relative number of CS and HS chains. This is consistent with the essential role of GlcAT-I in proteoglycan synthesis as the last step in linker synthesis before its division into CS, DS, and HS. Thus, any type of the affected GAG chains (CS, DS, or HS) may contribute to the characteristic symptoms of the patients.

Another step in linker synthesis, the addition of the second galactose residue, is affected in progeroid type Ehlers-Danlos syndrome (EDS progeroid form [MIM 130070]).[36–38] The phenotypic overlap with the family described here includes multiple joint dislocations, growth delay, skeletal malformations, and hypomineralization (osteopenia). Considerable overlap is also apparent with defects in another downstream enzyme which is essential for CS synthesis, chondroitin 6-*O*-sulfotransferase-1 (C6ST1 [MIM 603799]). Mutations in the gene carbohydrate sulfotransferase 3 (*CHST3* [MIM 603799]), coding for C6ST1, were shown to cause autosomal-recessive spondyloepiphyseal dysplasia with joint dislocations CHST3 type, a condition characterized by congenital joint dislocations (especially of the knee and elbow), club foot, vertebral changes (platyspondyly, intervertebral disc degeneration, scoliosis), short stature, arthritis, and heart defects (MIM 245600).[22,27,28] Mutations in chondroitin synthase 1 are associated with brachydactyly, mutations in the chondroitin beta-1,4-N-acetylgalactosaminyltransferase-1 with neuropathies.[39–41] A defect in the downstream enzyme in dermatan sulfate synthesis (dermatan 4-*O*-sulfotransferase 1, D4ST1, encoded by the gene carbohydrate sulfotransferase 14, *CHST14* [MIM 608429]) results in adducted thumb-clubfoot syndrome (ATCS [MIM 601776]), as well as a subtype of Ehlers-Danlos syndrome (EDS, musculocontractural type [MIM 601776]).[29,31] D4ST1 defects lead to a reduction in DS chains. Lack of DS chains was shown to impair the interaction with collagen to form collagen bundles.[31] Thus, proteoglycans devoid of DS chains may explain symptoms such as skin and joint laxity as well as tissue fragility. GlcAT-I defects also affect DS chains and accordingly symptoms of patients with GlcAT-I mutations overlap with these other clinical entities. However, defective linker synthesis additionally affects CS and HS proteoglycans.

We report a disease-causing mutation resulting in a defect terminal step of tetrasaccharide linkage region of proteoglycans synthesis. The phenotypes we observed in the affected individuals, namely joint dislocations, congenital heart defects, and short stature, overlap with symptoms seen in progeroid type EDS and in patients with spondyloepiphyseal dysplasia with congenital joint dislocations, CHST3 type. These findings suggest that proteoglycan synthesis pathway mutations may be responsible for atypical connective tissue disorders that feature joint dislocations, joint laxity, and congenital heart disease.

All patients described had congenital heart disease in various forms: mitral valve prolapse, bicuspid aortic valve with aortic root dilatation, ventricular septal defect, and atrial septal defect. Defects of heart valves are one of the most common inborn malformations. Among them, bicuspid aortic valve (BAV) is most frequent with a prevalence of 1%–2% in newborns.[42] Bicuspid aortic valves feature a significantly increased risk of life-threatening late complications such as aortic root dilatation, dissection of the aorta, and stenosis or insufficiency of the aortic valve with subsequent heart failure. In contrast to other congenital heart defects where already multiple genes were found to be involved, the genetic etiology of bicuspid

aortic valve remained mostly unresolved.[42,43] So far only one gene, *NOTCH1* (MIM 190198), was described for bicuspid aortic valve.[44] Thus, to the best of our knowledge, GlcAT-I defects appear to be the second gene pathogenetically related to this frequent and clinically relevant heart defect.

Our findings show that mutations affecting the proteoglycan linker region cause another subtype of connective tissue disorders and suggest pathogenetic relevance for a spectrum of congenital heart defects, including bicuspid aortic valves.

Supplemental Data

Supplemental Data include seven figures and two tables and can be found with this article online at http://www.cell.com/AJHG/.

Acknowledgments

We thank the family for their interest and participation. Friedrich Luft critically read the manuscript. S.B. received a scholarship from the Mongolian government and from the Charité Medical faculty. K.S. was supported by Grants-in-aid for Scientific Research B (20390019) and the Matching Program for Innovations in Future Drug Discovery and Medical Care from the Ministry of Education, Culture, Sports, Science, and Technology of Japan (MEXT). S.M. was supported by Grants-in-Aid for regional R&D Proposal-Based Program from Northern Advancement Center for Science & Technology of Hokkaido, and Grants-in-Aid for Young Scientists (B) 23790066 from Japan Society for the Promotion of Science, Japan. K.H. was supported by the Deutsche Forschungsgemeinschaft (DFG, SFB 577, project A4) and is a recipient of a Rahel Hirsch Fellowship, provided by the Charité Medical Faculty. S.B. dedicates this work to her father, Baasanjav Tseveen. S.B. genotyped the family for fine mapping and resequenced candidate genes. She and B.F. performed immunostaining, western blot, and quantitative PCR. L.A., B.R.A., S.A.A.A., and R.L. examined the patients. L.A., R.L., K.H., S.M., and D.H. compared phenotypes and analyzed the X-rays. C.B. and P.N. performed the Affymetrix SNP genotyping. Linkage analyses were run by K.H., T.H.L., and G.N. B.R.A. performed database searches identifying B3GAT3 as a candidate. Protein modeling was done by V.C., D.S., and J.G.G. T.H., S.M., and K.S. performed proteoglycan and GlcAT-I assays. K.H. supervised the project and wrote the manuscript. All authors edited and confirmed the manuscript.

Received: February 9, 2011
Revised: April 14, 2011
Accepted: May 16, 2011
Published online: July 14, 2011

Web Resources

The URLs for data presented herein are as follows:

Online Mendelian Inheritance in Man (OMIM), http://www.omim.org
PyMol, http://www.pymol.org
RCSC protein data bank, http://www.rcsb.org/pdb/home/home.do

References

1. Bulik, D.A., Wei, G., Toyoda, H., Kinoshita-Toyoda, A., Waldrip, W.R., Esko, J.D., Robbins, P.W., and Selleck, S.B. (2000). sqv-3, -7, and -8, a set of genes affecting morphogenesis in *Caenorhabditis elegans*, encode enzymes required for glycosaminoglycan biosynthesis. Proc. Natl. Acad. Sci. USA *97*, 10838–10843.
2. Sugahara, K., Mikami, T., Uyama, T., Mizuguchi, S., Nomura, K., and Kitagawa, H. (2003). Recent advances in the structural biology of chondroitin sulfate and dermatan sulfate. Curr. Opin. Struct. Biol. *13*, 612–620.
3. Haltiwanger, R.S., and Lowe, J.B. (2004). Role of glycosylation in development. Annu. Rev. Biochem. *73*, 491–537.
4. Häcker, U., Nybakken, K., and Perrimon, N. (2005). Heparan sulphate proteoglycans: The sweet side of development. Nat. Rev. Mol. Cell Biol. *6*, 530–541.
5. Berninsone, P.M. (2006). Carbohydrates and glycosylation. WormBook *18*, 1–22.
6. Franks, D.M., Izumikawa, T., Kitagawa, H., Sugahara, K., and Okkema, P.G. (2006). *C. elegans* pharyngeal morphogenesis requires both de novo synthesis of pyrimidines and synthesis of heparan sulfate proteoglycans. Dev. Biol. *296*, 409–420.
7. Bishop, J.R., Schuksz, M., and Esko, J.D. (2007). Heparan sulphate proteoglycans fine-tune mammalian physiology. Nature *446*, 1030–1037.
8. Sugahara, K., and Mikami, T. (2007). Chondroitin/dermatan sulfate in the central nervous system. Curr. Opin. Struct. Biol. *17*, 536–545.
9. Izumikawa, T., Kanagawa, N., Watamoto, Y., Okada, M., Saeki, M., Sakano, M., Sugahara, K., Sugihara, K., Asano, M., and Kitagawa, H. (2010). Impairment of embryonic cell division and glycosaminoglycan biosynthesis in glucuronyltransferase-I-deficient mice. J. Biol. Chem. *285*, 12190–12196.
10. Dai, J., and Rabie, A.B. (2007). VEGF: An essential mediator of both angiogenesis and endochondral ossification. J. Dent. Res. *86*, 937–950.
11. Stringer, S.E. (2006). The role of heparan sulphate proteoglycans in angiogenesis. Biochem. Soc. Trans. *34*, 451–453.
12. Chan, C.K., Rolle, M.W., Potter-Perigo, S., Braun, K.R., Van Biber, B.P., Laflamme, M.A., Murry, C.E., and Wight, T.N. (2010). Differentiation of cardiomyocytes from human embryonic stem cells is accompanied by changes in the extracellular matrix production of versican and hyaluronan. J. Cell. Biochem. *111*, 585–596.
13. Pilia, G., Hughes-Benzie, R.M., MacKenzie, A., Baybayan, P., Chen, E.Y., Huber, R., Neri, G., Cao, A., Forabosco, A., and Schlessinger, D. (1996). Mutations in *GPC3*, a glypican gene, cause the Simpson-Golabi-Behmel overgrowth syndrome. Nat. Genet. *12*, 241–247.
14. Capurro, M.I., Li, F., and Filmus, J. (2009). Overgrowth of a mouse model of Simpson-Golabi-Behmel syndrome is partly mediated by Indian hedgehog. EMBO Rep. *10*, 901–907.
15. Sugahara, K., and Kitagawa, H. (2000). Recent advances in the study of the biosynthesis and functions of sulfated glycosaminoglycans. Curr. Opin. Struct. Biol. *10*, 518–527.
16. Prydz, K., and Dalen, K.T. (2000). Synthesis and sorting of proteoglycans. J. Cell Sci. *113*, 193–205.
17. Guérardel, Y., Balanzino, L., Maes, E., Leroy, Y., Coddeville, B., Oriol, R., and Strecker, G. (2001). The nematode *Caenorhabditis elegans* synthesizes unusual O-linked glycans: Identification of glucose-substituted mucin-type O-glycans and short chondroitin-like oligosaccharides. Biochem. J. *357*, 167–182.

18. Hoffmann, K., and Lindner, T.H. (2005). easyLINKAGE-Plus—Automated linkage analyses using large-scale SNP data. Bioinformatics *21*, 3565–3567.
19. Lindner, T.H., and Hoffmann, K. (2005). easyLINKAGE: A PERL script for easy and automated two-/multi-point linkage analyses. Bioinformatics *21*, 405–407.
20. Hoffmann, K., Dreger, C.K., Olins, A.L., Olins, D.E., Shultz, L.D., Lucke, B., Karl, H., Kaps, R., Müller, D., Vayá, A., et al. (2002). Mutations in the gene encoding the lamin B receptor produce an altered nuclear morphology in granulocytes (Pelger-Huët anomaly). Nat. Genet. *31*, 410–414.
21. Kitagawa, H., Tone, Y., Tamura, J., Neumann, K.W., Ogawa, T., Oka, S., Kawasaki, T., and Sugahara, K. (1998). Molecular cloning and expression of glucuronyltransferase I involved in the biosynthesis of the glycosaminoglycan-protein linkage region of proteoglycans. J. Biol. Chem. *273*, 6615–6618.
22. van Roij, M.H., Mizumoto, S., Yamada, S., Morgan, T., Tan-Sindhunata, M.B., Meijers-Heijboer, H., Verbeke, J.I., Markie, D., Sugahara, K., and Robertson, S.P. (2008). Spondyloepiphyseal dysplasia, Omani type: further definition of the phenotype. Am. J. Med. Genet. A *146A*, 2376–2384.
23. Tone, Y., Kitagawa, H., Imiya, K., Oka, S., Kawasaki, T., and Sugahara, K. (1999). Characterization of recombinant human glucuronyltransferase I involved in the biosynthesis of the glycosaminoglycan-protein linkage region of proteoglycans. FEBS Lett. *459*, 415–420.
24. Ouzzine, M., Gulberti, S., Levoin, N., Netter, P., Magdalou, J., and Fournel-Gigleux, S. (2002). The donor substrate specificity of the human beta 1,3-glucuronosyltransferase I toward UDP-glucuronic acid is determined by two crucial histidine and arginine residues. J. Biol. Chem. *277*, 25439–25445.
25. Wei, G., Bai, X., and Esko, J.D. (2004). Temperature-sensitive glycosaminoglycan biosynthesis in a Chinese hamster ovary cell mutant containing a point mutation in glucuronyltransferase I. J. Biol. Chem. *279*, 5693–5698.
26. Unger, S., Lausch, E., Rossi, A., Mégarbané, A., Sillence, D., Alcausin, M., Aytes, A., Mendoza-Londono, R., Nampoothiri, S., Afroze, B., et al. (2010). Phenotypic features of carbohydrate sulfotransferase 3 (CHST3) deficiency in 24 patients: congenital dislocations and vertebral changes as principal diagnostic features. Am. J. Med. Genet. A. *152A*, 2543–2549.
27. Hermanns, P., Unger, S., Rossi, A., Perez-Aytes, A., Cortina, H., Bonafé, L., Boccone, L., Setzu, V., Dutoit, M., Sangiorgi, L., et al. (2008). Congenital joint dislocations caused by carbohydrate sulfotransferase 3 deficiency in recessive Larsen syndrome and humero-spinal dysostosis. Am. J. Hum. Genet. *82*, 1368–1374.
28. Thiele, H., Sakano, M., Kitagawa, H., Sugahara, K., Rajab, A., Höhne, W., Ritter, H., Leschik, G., Nürnberg, P., and Mundlos, S. (2004). Loss of chondroitin 6-*O*-sulfotransferase-1 function results in severe human chondrodysplasia with progressive spinal involvement. Proc. Natl. Acad. Sci. USA *101*, 10155–10160.
29. Dündar, M., Müller, T., Zhang, Q., Pan, J., Steinmann, B., Vodopiutz, J., Gruber, R., Sonoda, T., Krabichler, B., Utermann, G., et al. (2009). Loss of dermatan-4-sulfotransferase 1 function results in adducted thumb-clubfoot syndrome. Am. J. Hum. Genet. *85*, 873–882.
30. Malfait, F., Syx, D., Vlummens, P., Symoens, S., Nampoothiri, S., Hermanns-Lê, T., Van Laer, L., and De Paepe, A. (2010). Musculocontractural Ehlers-Danlos Syndrome (former EDS type VIB) and adducted thumb clubfoot syndrome (ATCS) represent a single clinical entity caused by mutations in the dermatan-4-sulfotransferase 1 encoding *CHST14* gene. Hum. Mutat. *31*, 1233–1239.
31. Miyake, N., Kosho, T., Mizumoto, S., Furuichi, T., Hatamochi, A., Nagashima, Y., Arai, E., Takahashi, K., Kawamura, R., Wakui, K., et al. (2010). Loss-of-function mutations of CHST14 in a new type of Ehlers-Danlos syndrome. Hum. Mutat. *31*, 966–974.
32. Pedersen, L.C., Tsuchida, K., Kitagawa, H., Sugahara, K., Darden, T.A., and Negishi, M. (2000). Heparan/chondroitin sulfate biosynthesis. Structure and mechanism of human glucuronyltransferase I. J. Biol. Chem. *275*, 34580–34585.
33. Negishi, M., Dong, J., Darden, T.A., Pedersen, L.G., and Pedersen, L.C. (2003). Glucosaminylglycan biosynthesis: What we can learn from the X-ray crystal structures of glycosyltransferases GlcAT1 and EXTL2. Biochem. Biophys. Res. Commun. *303*, 393–398.
34. Ouzzine, M., Antonio, L., Burchell, B., Netter, P., Fournel-Gigleux, S., and Magdalou, J. (2000). Importance of histidine residues for the function of the human liver UDP-glucuronosyltransferase UGT1A6: Evidence for the catalytic role of histidine 370. Mol. Pharmacol. *58*, 1609–1615.
35. Gilchrist, A., Au, C.E., Hiding, J., Bell, A.W., Fernandez-Rodriguez, J., Lesimple, S., Nagaya, H., Roy, L., Gosline, S.J., Hallett, M., et al. (2006). Quantitative proteomics analysis of the secretory pathway. Cell *127*, 1265–1281.
36. Kresse, H., Rosthøj, S., Quentin, E., Hollmann, J., Glössl, J., Okada, S., and Tønnesen, T. (1987). Glycosaminoglycan-free small proteoglycan core protein is secreted by fibroblasts from a patient with a syndrome resembling progeroid. Am. J. Hum. Genet. *41*, 436–453.
37. Okajima, T., Fukumoto, S., Furukawa, K., and Urano, T. (1999). Molecular basis for the progeroid variant of Ehlers-Danlos syndrome. Identification and characterization of two mutations in galactosyltransferase I gene. J. Biol. Chem. *274*, 28841–28844.
38. Faiyaz-Ul-Haque, M., Zaidi, S.H., Al-Ali, M., Al-Mureikhi, M.S., Kennedy, S., Al-Thani, G., Tsui, L.C., and Teebi, A.S. (2004). A novel missense mutation in the galactosyltransferase-I (*B4GALT7*) gene in a family exhibiting facioskeletal anomalies and Ehlers-Danlos syndrome resembling the progeroid type. Am. J. Med. Genet. A *128A*, 39–45.
39. Li, Y., Laue, K., Temtamy, S., Aglan, M., Kotan, L.D., Yigit, G., Canan, H., Pawlik, B., Nürnberg, G., Wakeling, E.L., et al. (2010). Temtamy preaxial brachydactyly syndrome is caused by loss-of-function mutations in chondroitin synthase 1, a potential target of BMP signaling. Am. J. Hum. Genet. *87*, 757–767.
40. Tian, J., Ling, L., Shboul, M., Lee, H., O'Connor, B., Merriman, B., Nelson, S.F., Cool, S., Ababneh, O.H., Al-Hadidy, A., et al. (2010). Loss of CHSY1, a secreted FRINGE enzyme, causes syndromic brachydactyly in humans via increased NOTCH signaling. Am. J. Hum. Genet. *87*, 768–778.
41. Saigoh, K., Izumikawa, T., Koike, T., Shimizu, J., Kitagawa, H., and Kusunoki, S. (2011). Chondroitin beta-1,4-*N*-acetylgalactosaminyltransferase-1 missense mutations are associated with neuropathies. J. Hum. Genet. *56*, 143–146.
42. Bruneau, B.G. (2008). The developmental genetics of congenital heart disease. Nature *451*, 943–948.

43. Leong, F.T., Freeman, L.J., and Keavney, B.D. (2009). Fresh fields and pathways new: Recent genetic insights into cardiac malformation. Heart *95*, 442–447.
44. Garg, V., Muth, A.N., Ransom, J.F., Schluterman, M.K., Barnes, R., King, I.N., Grossfeld, P.D., and Srivastava, D. (2005). Mutations in NOTCH1 cause aortic valve disease. Nature *437*, 270–274.
45. Tone, Y., Pedersen, L.C., Yamamoto, T., Izumikawa, T., Kitagawa, H., Nishihara, J., Tamura, J., Negishi, M., and Sugahara, K. (2008). 2-*o*-phosphorylation of xylose and 6-*o*-sulfation of galactose in the protein linkage region of glycosaminoglycans influence the glucuronyltransferase-I activity involved in the linkage region synthesis. J. Biol. Chem. *283*, 16801–16807.